# Multicolor fate mapping of Langerhans cell homeostasis

Clément Ghigo,[1,2,3,4] Isabelle Mondor,[1,2,3,4] Audrey Jorquera,[1,2,3,4] Jonathan Nowak,[1,2,3,4] Stephan Wienert,[5] Sonja P. Zahner,[6] Björn E. Clausen,[6,7] Hervé Luche,[8] Bernard Malissen,[1,2,3,4] Frederick Klauschen,[5] and Marc Bajénoff[1,2,3,4]

[1]Centre d'Immunologie de Marseille-Luminy (CIML), Aix-Marseille Université, UM2, 13288 Marseille, France
[2]Institut National de la Santé et de la Recherche Médicale (INSERM), U1104, 13288 Marseille, France
[3]Centre National de la Recherche Scientifique (CNRS), UMR7280, 13288 Marseille, France
[4]Aix-Marseille Univ (AMU), F-13284, 13288 Marseille, France
[5]Institute of Pathology, Charité Universitätsmedizin Berlin, 10117 Berlin, Germany
[6]Dept. of Immunology, Erasmus MC, University Medical Center, 3015 GE Rotterdam, The Netherlands
[7]Institute for Molecular Medicine, University Medical Center of the Johannes Gutenberg-University Mainz, 55131 Mainz, Germany
[8]INSERM US012/CNRS, AMU, Unité Mixte de Service 3367, 13288 Marseille, France

**Langerhans cells (LCs) constitute a network of immune sentinels in the skin epidermis that is seeded during embryogenesis. Whereas the development of LCs has been extensively studied, much less is known about the homeostatic renewal of adult LCs in "nonmanipulated" animals. Here, we present a new multicolor fluorescent fate mapping system and quantification approach to investigate adult LC homeostasis. This novel approach enables us to propose and provide evidence for a model in which the adult epidermal LC network is not formed by mature coequal LCs endowed with proliferative capabilities, but rather constituted by adjacent proliferative units composed of "dividing" LCs and their terminally differentiated daughter cells. Altogether, our results demonstrate the general utility of our novel fate-mapping system to follow cell population dynamics in vivo and to establish an alternative model for LC homeostasis.**

CORRESPONDENCE
M. Bajénoff:
bajenoff@ciml.univ-mrs.fr
OR
F. Klauschen:
Frederick.Klauschen@charite.de

Abbreviations used: EDU, 5-ethynyl-2′-deoxyuridine; ERT2, estrogen receptor T2; Flt3, fms-like tyrosine kinase 3 ligand; LC, Langerhans cell.

Cell division and proliferation are fundamental biological processes central to the development and homeostasis of all organisms. The recent development of multicolor fate-mapping systems based on the Cre-*loxP* system technology has created new tools to study cell dynamics in situ. However, these reporter mice have only been reported to work when combined with mouse strains carrying Cre-inducible systems such as the widely used tamoxifen-inducible ones (Snippert et al., 2010; Tabansky et al., 2013).

Epidermal LCs represent a subpopulation of dendritic cells that reside in the skin epidermis and continuously migrate to the proximal draining lymph node to present captured antigens to immune cells in both inflammatory and steady-state conditions (Merad et al., 2008). Although DCs and LCs appear to be functionally related, they do not share differentiation and homeostatic features. The development and homeostasis of DCs are regulated by fms-like tyrosine kinase 3 ligand (Flt-3L) but do not not require IL-34 or TGF-β1 cytokines (Borkowski et al., 1996; McKenna et al., 2000). On the contrary, the development and homeostasis of LCs are severely impaired in the absence of IL-34 or TGF-β1 but is unaffected in Flt-3L–deficient mice (Borkowski et al., 1997; Kel et al., 2010; Greter et al., 2012; Wang et al., 2012).

Despite their developmental differences, LCs and DCs face a similar challenge at steady-state conditions. Both cell networks need to maintain a fixed number of cells despite their short lifespan (DCs) or continuous emigration (LCs). While the rapid turnover of lymphoid DCs is counterbalanced by the sustained input of peripheral blood precursors (Liu et al., 2007), the emigration of LCs is thought to be compensated by the local proliferation of mature LCs





The Journal of Experimental Medicine

(Chorro et al., 2009; Merad et al., 2002). However, in absence of an appropriate model to study LC homeostasis in nonmanipulated animals, direct evidence supporting this assumption is critically lacking.

Here, we present a novel multicolor fate mapping mouse model compatible with any constitutively Cre-expressing mouse strain and its application to unravel LC homeostasis. We provide evidence that the adult epidermal LC network is not formed by mature coequal LCs endowed with proliferative capabilities but rather constituted by adjacent proliferative units composed of dividing LCs and their terminally differentiated daughter cells.

## RESULTS AND DISCUSSION

We designed a transgenic mouse dubbed "Ubow," in which the Brainbow 1.0L construct that allows for combinatorial expression of three spectrally different fluorescent reporter proteins was placed under control of the strong human Ubiquitin-C promoter (Fig. 1 A; Livet et al., 2007). As recombination of the Brainbow 1.0L cassette is caused by a Cre-mediated excision, any Ubow cell that constitutively co-expresses Cre performs a single and definitive recombination event. In other words, any Ubow cell constitutively expressing Cre acquires a specific color for its entire lifespan, a unique feature distinct from the related Confetti mouse in which constitutively Cre-expressing cells are expected to constantly switch their colors (Snippert et al., 2010).

Analysis of various organs harvested from Ubow mice revealed that all cells strongly express dTomato in the absence of CFP and YFP (unpublished data). To trigger the recombination of the Ubow construct in all cells of the animal, we crossed Ubow$^{+/+}$ mice to tamoxifen Cre-inducible Ubiquitin-Cre estrogen receptor T2 (ERT2) mice (hereafter referred to as Ubow-CreERT2). Ubow-CreERT2 mice bearing two copies of the Ubow cassette were treated with tamoxifen and analyzed 3 wk later (Ruzankina et al., 2007; Fig. 1 B). As expected, the presence of two copies of the Ubow construct allowed for combinatorial expression of fluorescent proteins in all the harvested organs of the mice. Importantly, analysis of their gut revealed the presence of monocolored columns of enterocytes, confirming the efficacy of the Ubow mouse to map the fate of dividing cells.

Having demonstrated the ability of the Ubow mouse to track the behavior of transiently Cre-expressing cells, we tested its capacity to map the fate of constitutively Cre-expressing cells. We focused our attention on LCs, a population of long-lived, skin-resident DCs that continuously migrate from the epidermis to the draining lymph nodes (LNs). As LCs are not renewed from circulating progenitors, homeostatic LC emigration is thought to be compensated for by the local proliferation of mature LCs (Merad et al., 2002, 2008; Chorro et al., 2009). In other words, terminally differentiated epidermal LCs are believed to continuously replenish the empty "slots" created by emigrating LCs. However, this dogmatic view has never been experimentally demonstrated.

To map the fate of LCs, Ubow mice were crossed to Langerin-Cre (Lang-Cre) knock-in mice in which LCs express the Cre recombinase (Zahner et al., 2011). As expected, Langerin$^+$ CD11b$^+$ LCs isolated from the skin epidermis of Lang-Cre$^-$ Ubow$^{+/-}$ mice expressed dTomato in the absence of CFP or YFP, whereas virtually all epidermal LCs isolated from Lang-Cre$^+$ Ubow$^{+/-}$ mice expressed CFP or YFP (but never both) in the absence of dTomato (Fig. 1 C). Despite the fact that the recombination events leading to CFP and YFP expression are purely stochastic in the Brainbow 1.0L construct, we consistently observed a bias toward YFP expression (79% YFP, 19% CFP) in LCs isolated from Lang-Cre$^+$ Ubow$^{+/-}$ mice. Such bias was also observed in B cells and myeloid cells of Ubow mice crossed to reporter mice in which those cell types specifically express Cre (unpublished data), suggesting that Cre binds canonical and mutant *loxP* sequences with different affinities.

We next investigated the arrangement of colored LCs in the skin epidermis of adult Lang-Cre$^+$ Ubow$^{+/-}$ mice. We reasoned that if epidermal migrating LCs were replaced by neighboring LCs, the distribution of CFP$^+$ and YFP$^+$ LCs should be random in the epidermis, as both colored populations should randomly replace each other. On the contrary, if few LCs were constantly renewing their neighbors or if all mature LCs had the capacity to stochastically undergo few divisions, CFP$^+$ and YFP$^+$ LCs should no longer be randomly distributed but rather clustered in monocolored foci, each composed of one dividing LC and its progeny. Skin-draining LNs and epidermis of adult Lang-Cre$^+$ Ubow$^{+/-}$ mice were harvested and analyzed by confocal microscopy (Fig. 1 D). As expected, skin-derived CFP$^+$ and YFP$^+$ Langerin$^+$ cells were randomly distributed in the draining LNs (Fig. 1 D, left). Epidermal CFP$^+$ and YFP$^+$ LCs were not randomly distributed in the epidermal skin, but assembled in monocolored foci (Fig. 1 D, right). To confirm this visual impression, we quantified the clustering index of CFP$^+$ LCs that represented only ~20% of all LCs (Fig. 1 E). To achieve this, we developed the analysis software "ClusterQuant," in which the different cell types (CFP$^+$ and YFP$^+$ LCs) are manually labeled within microscopic images. Subsequently, automatic computation of the corresponding Voronoi diagrams was combined with Monte Carlo simulations to obtain a quantitative statistical measure of the spatial distribution (i.e., cluster formation or diffuse cell spreading) of the LCs (see Materials and methods and Fig. S1 for technical details). ClusterQuant is specifically designed for the statistical analysis of spatial cell distributions and can be applied to any multicolor fate mapping system. The results show with high significance that CFP$^+$ LCs form clusters (mean cluster size = 5.9 cells; median significance of cluster formation, $P < 10^{-9}$; Fig. 1 E). We then sought to analyze the skin epidermis of Lang-Cre$^+$ Ubow$^{+/+}$ mice that express two copies of the Ubow transgene. In these mice, LCs could be CFP$^{2+}$, YFP$^{2+}$ or CFP$^+$YFP$^+$. As CFP$^+$ LCs represent only 20% of all LCs in Lang-Cre$^+$ Ubow$^{+/-}$ mice, we expected the frequency of CFP$^{2+}$ LCs in Lang-Cre$^+$ Ubow$^{+/+}$ mice to be approximately 4%. In such case, the recombination bias observed

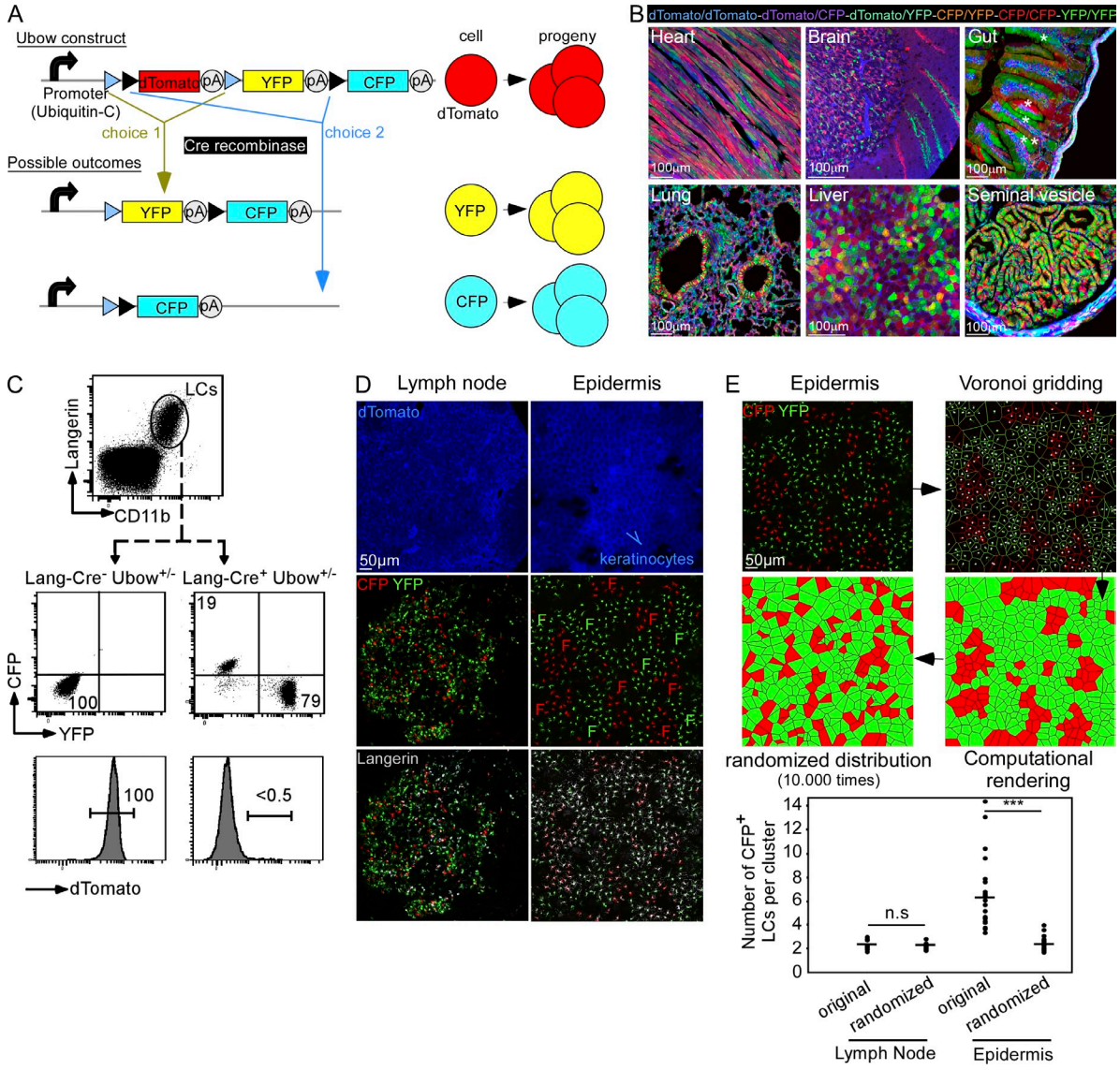


**Figure 1. Multicolor fate mapping of LCs.** (A) In the Ubow construct, the Brainbow 1.0L cassette has been placed under the control of the human Ubiquitin-C promoter, ensuring that all cells strongly express the construct. Before Cre action, cells express dTomato in the absence of CFP and YFP. Upon Cre activity, cells lose dTomato expression and stochastically acquire YFP (choice 1) or CFP (choice 2). This choice is definitive and transmittable to the cell's progeny. (B) Confocal pictures of various organs of a Ubow$^{+/+}$-CreERT2 mouse harvested 1 mo after tamoxifen treatment. Note the monocolored columns of enterocytes in the gut (*). Data are representative of two independent experiments (two mice per experiment). (C) Flow cytometric analysis of Langerin$^{+}$ CD11b$^{+}$ LCs harvested from the epidermis of Lang-Cre$^{+}$ Ubow$^{+/-}$ mice. (D) Ear epidermis and skin-draining LNs of Lang-Cre$^{+}$ Ubow$^{+/-}$ mice were stained for Langerin expression and analyzed by confocal microscopy. "F" indicates the location of monocolored foci of LCs. (E) All confocal pictures of epidermal LCs similar to the ones imaged in D were processed to generate Voronoi-tessellated pictures (see Materials and methods and Fig. S1) amenable to computational simulation. The numbers of CFP$^{+}$ LCs per cluster were then compared with Monte Carlo–simulated datasets in which the same LC populations were randomly distributed (1 simulation displayed out of 10.000). ***, $P < 10^{-9}$. Data are representative of five different experiments (two mice per experiment) in C–E. Bars show the medians.

in the Ubow mouse would represent a unique advantage to track the behavior of very few cells belonging to a much larger population. Flow cytometric analysis of CFP$^{2+}$,YFP$^{2+}$, and CFP$^{+}$YFP$^{+}$ epidermal LCs isolated from Lang-Cre$^{+}$ Ubow$^{+/+}$ mice confirmed that these three colored populations appeared at the expected frequencies (Fig. 2 A). Because we observed the same ratios in two other constitutively Cre-expressing strains of mice crossed to Ubow$^{+/+}$ mice (unpublished data), we concluded that the fate of this rare CFP$^{2+}$ population could be extrapolated to the entire population of colored cells. We thus assessed the distribution of CFP$^{2+}$ LCs in the skin epidermis of Lang-Cre$^{+}$ Ubow$^{+/+}$ mice and observed that despite their paucity, these cells were nonrandomly gathered in foci (Fig. 2, B and C), confirming our observations

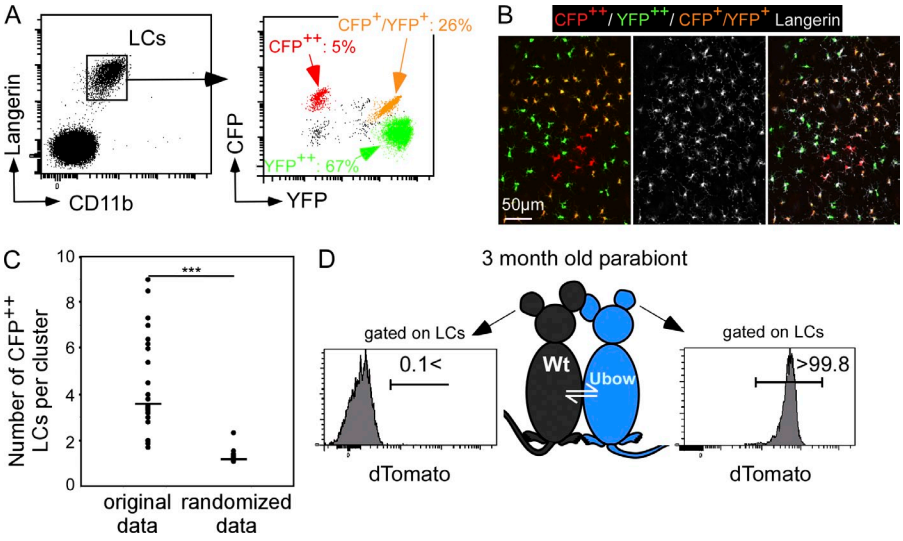


**Figure 2. LC foci rely on tissue-resident LCs.** Flow cytometric (A) and confocal (B and C) analyses of LCs harvested from the epidermis of Lang-Cre$^{+}$ Ubow$^{+/+}$ mice. Data are representative of five independent experiments (two mice per experiment). ***, $P < 10^{-9}$. (D) Nonfluorescent WT mice were joined surgically with Ubow$^{+/-}$ mice to create parabiotic mice. 3 mo later, the colors (and thus the origin) of Langerin$^{+}$ CD11b$^{+}$ LCs harvested from the ear epidermis of both mice were assessed by flow cytometry. Data are representative of three different parabiotic pairs.

in the Lang-Cre$^{+}$ Ubow$^{+/-}$ mice. Finally, parabiotic mice confirmed the previously reported absence of contribution of BM-derived cells to LC homeostasis (Fig. 2 D; Merad et al., 2002; Chorro et al., 2009). Altogether, these results suggested that the adult LC network is constituted by contiguous LC-proliferative units composed of tissue-resident dividing LCs and their daughter cells.

Because LCs undergo a burst of proliferation in newborn mice that could generate self-renewing LC clusters in adult mice (Chorro et al., 2009), we designed an experimental protocol in which recombination of the Ubow construct could be triggered in adult LCs. To this aim, we took advantage of Ubow-CreERT2 mice. We reasoned that upon tamoxifen injection in adult Ubow-CreERT2 mice, some LCs should stochastically express CFP or YFP, whereas the remaining ones should maintain the expression of dTomato. Such random acquisition of colors would initially create a mosaic of colored LCs a few days later. If LCs were coequal and able to replace their immediate emigrating neighbors, CFP$^{+}$, YFP$^{+}$, and dTomato$^{+}$ LCs should replace each other at the same rate, preventing the apparition of foci of colored cells. On the contrary, if only certain subsets of LCs were in charge of renewing their neighbors and/or if mature LCs could be stochastically triggered to undergo a certain number of divisions, foci of monocolored LCs should develop over time from such dividing LCs, whereas isolated terminally differentiated cells should progressively disappear.

As adult LCs display a slow turnover (Merad et al., 2002; Vishwanath et al., 2006), adult Ubow$^{+/-}$ and Ubow-CreERT2 mice were treated with tamoxifen (or vehicle), and their ear epidermis was analyzed 1, 5, and 15 wk later (Fig. 3 A). No recombination was observed in Ubow mice treated with tamoxifen or Ubow-CreERT2 mice treated with vehicle (unpublished data). On the contrary, ∼10% of adult LCs expressed CFP$^{+}$ or YFP$^{+}$ in Ubow-CreERT2 mice treated with tamoxifen (unpublished data). As expected, CFP$^{+}$ and YFP$^{+}$ LCs were randomly distributed in the epidermis of tamoxifen-treated Ubow-CreERT2 mice 1 wk after tamoxifen injection (Fig. 3 B). Analysis at later time points indicated that this initial mosaic of CFP$^{+}$ and YFP$^{+}$ LCs progressively disappeared and was replaced by rare foci of monocolored LCs (Fig. 3 B) similar to the ones observed in constitutive Lang-Cre$^{+}$ Ubow$^{+/-}$ mice. Quantification indicated an increase in the average cluster size from 1.6 cells (1 wk, Monte Carlo simulation-derived significance of clustering, $P = 0.25$), via 2.9 cells (1 mo, $P < 0.0001$) to 5.4 cells per cluster (3 mo, $P < 0.00001$) for CFP$^{+}$ LCs. Such reorganization was associated with a drastic diminution of isolated CFP$^{+}$ and YFP$^{+}$ LCs and a concomitant increase in the number of LCs per foci; Fig. 3 C).

We next sought to phenotype dividing LCs. To this aim, we injected 5-ethynyl-2′-deoxyuridine (EDU), a thymidine analogue, into adult mice and analyzed the phenotype of dividing LCs 14 h later by flow cytometry. Within this period, only ∼1% of LCs incorporated EDU (Fig. 3 D). Interestingly, EDU$^{+}$ Langerin$^{+}$ LCs were highly enriched (75%) in the CD11b$^{lo}$ MHC class II$^{lo}$ fraction as compared with EDU$^{-}$ Langerin$^{+}$ LCs (18%). Additional phenotyping indicated that CD11b$^{lo}$ MHC class II$^{lo}$ LCs represented 20% of all LCs and expressed lower levels of CD86 and Epcam as compared with the rest of the LC population (Fig. 3 E). As MHC class II and CD86 are typical LC activation markers (Carreno and Collins, 2002; Girolomoni et al., 1990), our observation suggested that these LCs (a) constituted the most immature fraction of LCs and (b) were endowed with higher but limited proliferative capacities. Although we cannot rule out the possibility that all LCs contribute to the maintenance of LC homeostasis, our results favor a model in which few immature LCs are in charge of replacing neighboring emigrating LCs, and thus responsible for the maintenance of LC proliferative units. Such immature dividing LCs might be progenitors or might derive from the general LC population by some yet unknown mechanism.

BM-derived myeloid cells slowly replenish the epidermis of LC-depleted mice in clusters (Ginhoux et al., 2006; Poulin et al., 2007; Nagao et al., 2012). However, several studies indicated that the myeloid contribution to LC dynamics is

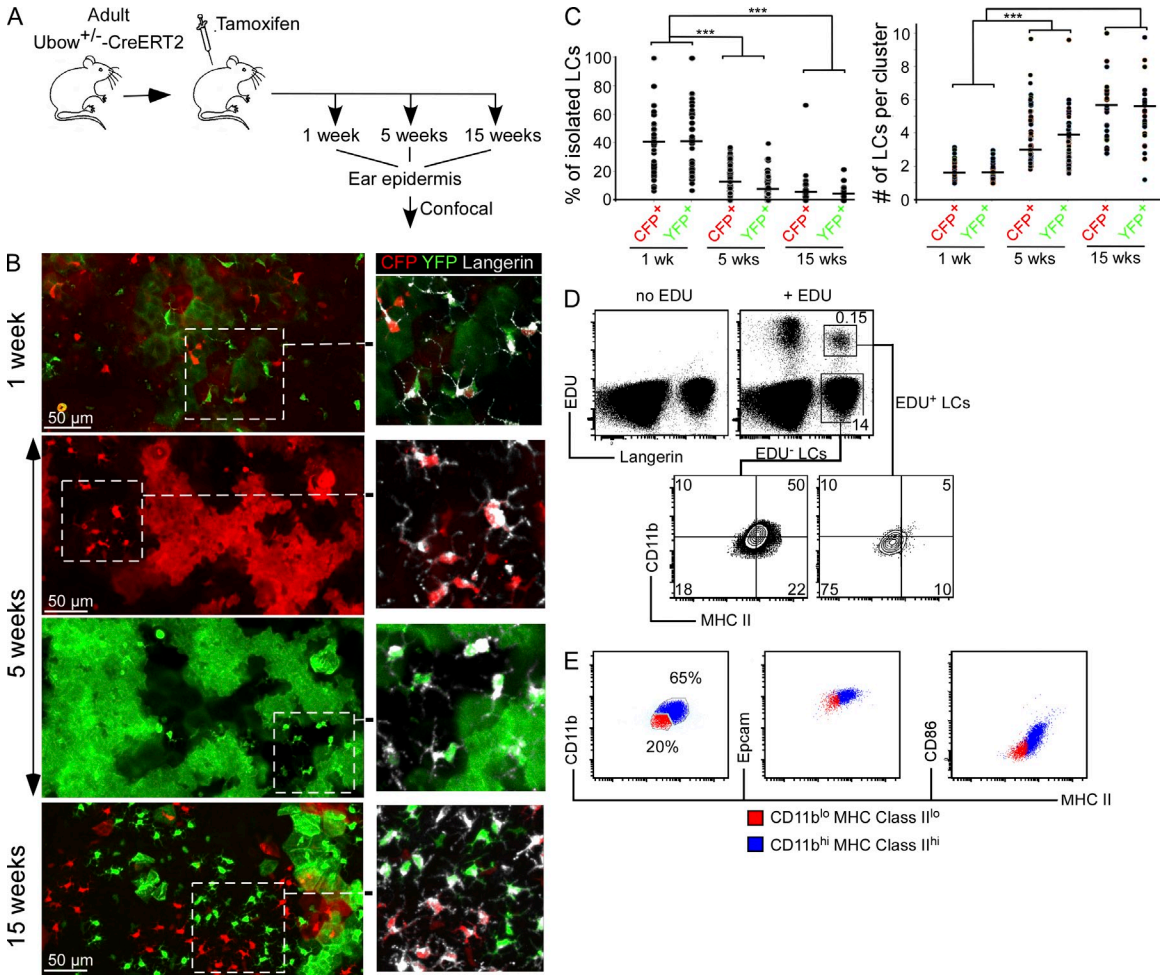


**Figure 3. LC foci are dynamic structures.** (A) Experimental protocol used to trigger recombination of the Ubow construct in adult LCs. (B) Ear epidermis of Ubow-CreERT2 mice were harvested 1, 5, or 15 wk after tamoxifen treatment, stained for Langerin expression, and analyzed by confocal microscopy. (C) Percentages of isolated CFP+ and YFP+ LCs and numbers of CFP+ and YFP+ LCs per LC foci. ***, $P < 10^{-4}$. Bars show the medians. Data are representative of three independent experiments (six mice per experiment) in B and C. (D) WT mice were injected or not with EDU. 14 h later, epidermal LCs were positively enriched with CD45 microbeads and stained for CD11b, Langerin, and EDU (D) or CD11b, MHC class II, Epcam, and CD86 (E) expression and analyzed by flow cytometry. Data are representative of three independent experiments (three mice per condition in each experiment).

extremely limited in other inflammatory models (Merad et al., 2002; Chorro et al., 2009), suggesting that this phenomenon may only occur when all tissue-resident LCs are eradicated by extreme means. We thus investigated the behavior of LCs in a "tape-stripping" model known to induce mild LC emigration while maintaining endogenous LCs (Holzmann et al., 2004). The left ears of WT mice were tape-stripped, and the right ones were untouched. 5 d later, EDU was injected into the mice and the percentage of EDU+ dividing LCs in both epidermises was assessed 14 h later by flow cytometry (Fig. 4 A). The results indicate that the mechanical disruption of the epidermis induced a robust proliferative response in LCs as compared with control epidermis (8 vs. 1% of EDU+ LCs). We then took advantage of BM chimeras to assess the capacity of BM-derived cells to migrate, proliferate, and generate LC foci in inflamed epidermis. Irradiated WT mice were reconstituted with BM cells isolated from Lang-Cre+ Ubow+/− or +/+ mice and submitted to the same tape-stripping protocol. To visualize the proliferative history of these BM-derived LCs, control and inflamed epidermis were harvested 3 wk after tape stripping. Flow cytometry analysis indicated that BM-derived LCs home to inflamed but not control epidermis and significantly accumulated in the LC network (Fig. 4 B), whereas confocal analysis revealed that these LCs associated in foci (Fig. 4 C).

These results indicate that upon inflammation, BM-derived cells are mobilized to replenish the LC network even in the presence of endogenous remaining LCs. They also demonstrate that BM-derived LCs assemble in proliferative units reminiscent of those generated by endogenous LCs at steady state.

In summary, we combined the ontogenic and homeostatic fate mapping capabilities of the Ubow mouse to investigate the cellular mechanisms that regulate the homeostatic renewal of the LC network and its replenishment after inflammation.

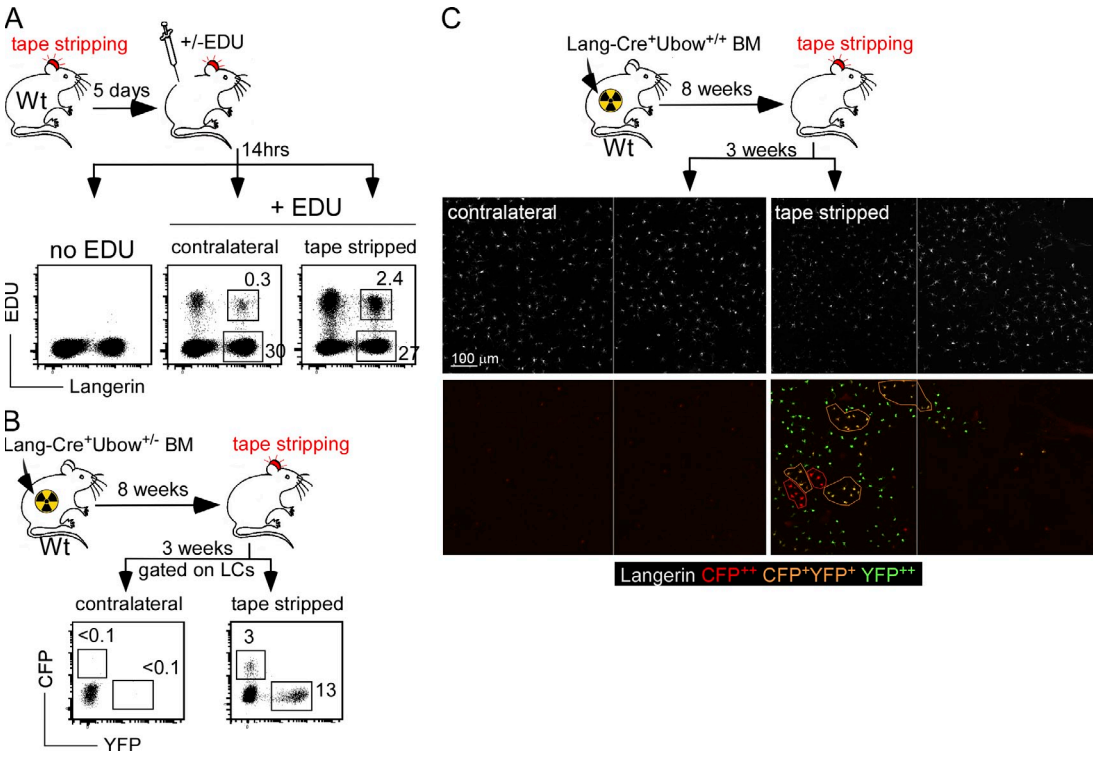


**Figure 4. Imaging LC behavior after inflammation.** The left ears of WT (A) chimeric mice reconstituted with Lang-Cre+ Ubow+/− (B) or Lang-Cre+ Ubow+/+ (C) BM cells were tape stripped, and the right ones were untouched. Mice were analyzed 5 or 21 d later. In the first protocol (A), EDU was injected in the mice 5 d after tape-stripping, and the percentages of EDU+ dividing LCs were assessed 14 h later by flow cytometry. Data are representative of three independent experiments (three mice per condition in each experiment). In the second protocol (B and C), we quantified the contribution (B) and the distribution (C) of BM-derived Langerin+ LCs in the control and inflamed epidermis 21 d after tape stripping. Circles point to monolored LC foci. Data are representative of three independent experiments (two mice per condition in each experiment).

We show for both scenarios that substitution of emigrating LCs leads to the formation of foci of LCs each originating from a single cell, therefore supporting models that either rely on the existence of a multitude of LC progenitors or mechanisms that enable subsets of LCs to acquire potentially transient and limited progenitor-like properties.

## MATERIALS AND METHODS

**Ethics statement.** All procedures performed on animals in this study have been approved by the animal ethics committee of Marseille (France).

**Mice.** C57BL/6J,Ubiquitin-CreERT2 mice (B6.Cg-Tg(UBC-cre/ERT2) 1Ejb/J, strain 8085) were purchased from The Jackson Laboratory. Ubow mice were generated in the Service des Animaux Transgéniques (SEAT; Orléans, France). All mice were on C57BL/6J background (>8 backcrosses) and maintained in the CIML animal facilities and used between 6 and 12 wk unless indicated in the text.

**Vector construction.** Genomic clones containing the human Ubiquitin C gene (UBC, ENSG00000150991) were purchased from Imagene. A 10-kb fragment was subcloned using DNA cloning by homologous recombination in *Escherichia coli* (ET recombination; Zhang et al., 2000) to prevent intercopy recombination. In brief, the minimal vector for Red/ET cloning (2.7 kb) was amplified using high-fidelity Taq polymerase from Roche and a pair of specific primers flanking the 10-kb promoter region of UBC gene: HL218: 5′-AATCATTTGGGTCAATATGTAATTTTCAGTGTTAGACTAGTAAATTGTCCGCTAAATTCTGGCCGTTTTTGGCTAGCCCTCGAGGGGGGGCCCGGTACC-3′ and HL219 5′-CTCC TGCCTCAGGCTCCTGAGTAGCTGGGATTACAGGCGTGCACCACTACGCCCAGCTAATTTTTGTATTTTTAG TAAGCGGCCGCCACCGCGGTGGAGC-3′. 300 ng of resulting plasmid were electroporated into competent BAC containing bacteria to proceed to ET cloning. Resulting subclones were tested for the presence of the recombinant construction (pMB-AW) by NheI restriction digest and sequencing. Release of a 9,257-kb indicator fragment revealed a correct integration. The Brainbow cassette 1.0 containing the array of fluorescent proteins (dTomato, mCerulean, and EYFP) was extracted from pCMV-Rainbow (Livet et al., 2007), as a 3.75-kb fragment upon NheI–SspI restriction digest and subcloned into NheI–SmaI of pX2-EGFP recipient plasmid (Irion et al., 2007). To maximize transgene expression level, a "Splice Donor-Intron-Splice Acceptor" cassette of 0.6 kb was extracted from pDOI5 by NheI–XbaI restriction digest (Kouskoff et al., 1993) and placed into the NheI site in front of the Brainbow cassette. The resulting plasmid (pMB-AY) was further digested by NheI–AscI and ligated to an 11.7-kb NheI–AscI fragment from pMB-AW. For hUbc-Rainbow transgenesis, the final vector (pMB-AZ) was digested with MluI to remove all residual bacterial sequences, and then injected into C57BL6/N oocyte. All vector maps and sequences can be provided upon request.

**Quantification of LC clustering.** The quantification and statistical analysis of the spatial distribution of LCs consists of three modules combined in the ClusterQuant software, which we developed with the CognitionMaster image analysis platform (http://sourceforge.net/projects/cognitionmaster/) based on C#/.NET (Wienert et al., 2013). Computations were performed

on standard hardware running Microsoft Windows 7 64-bit. In the first module, the different LC classes are defined using the Region-of-Interest plugin (ROImanager) of ClusterQuant/CognitionMaster, and the respective cells are labeled manually to obtain the cell center coordinate information for the subsequent processing step, in which the second module computes the two-dimensional Voronoi mesh based on the manually labeled cell centers. The resulting tessellation establishes the neighborhood relationships between the cells, which is used to evaluate the number of cells (of the same type) assembled in clusters and the respective cluster sizes. Although this step provides a robust and objective means of cell cluster quantification, it does not yet allow for an assessment of the (non)randomness of the spatial cell distribution/cluster formation. To achieve this, in the final step, we use Monte Carlo simulations based on the cell numbers present in the corresponding experimental image data. In the 10,000 simulation runs we perform for each experimental dataset, the same numbers of cells as in the real images are randomly distributed over the same image areas, and for each simulation run, the spatial statistics (Voronoi mesh, neighborhood, and cell cluster features) are computed in same way as for the experimentally obtained images. After all simulation runs are completed, we compare the results of the spatial statistics of the real and simulated data. The ratio between the number of simulations in which the average cluster size is larger than in the real data and the total number of Monte Carlo simulations (here: 10,000) yields the p-values, indicating the probability that an experimentally observed cluster formation may as well have been achieved by random cell distribution (Fig. S1). In addition to significance evaluation using Monte Carlo simulations for each dataset, we compared the cluster formation differences between the UbowCreERT2 at 1, 5, and 15 wk using standard *t* test statistics.

**Parabiosis.** 10-wk-old WT and Ubow$^{+/-}$ mice were surgically attached as previously described (Waskow, 2010). Parabionts were analyzed 3 mo later.

**BM chimeras.** Mice were γ-irradiated (twice with 500 rads) from an x-ray source and were reconstituted with at least 5 million BM cells. Chimeras were used at 8 wk after reconstitution.

**Tape-stripping of skin.** Mice were anesthetized with ketamine/xylazine. The dorsal side of the left ear was stripped by repeated application (15 times) of tape (1322-18 mm 3M comply indicator).

**Antibodies.** CD11b (M1/70), CD86 (GL1), MHC class I (M5/114.15.2), and Epcam (G8.8)-specific antibodies were purchased from BD. Anti-Langerin (929F3.01) was purchased from Dendritics. These antibodies were visualized by direct coupling to Pacific blue, allophycocyanin, or Alexa Fluor-488, -568, -647 antibodies (Life Technologies).

**Tamoxifen treatment.** Tamoxifen and corn oil were purchased from Sigma Aldrich. Tamoxifen (3 mg) was dissolved in corn oil and administered for 5 consecutive days i.p.

**Immunostaining.** Naired ears were divided in two leaflets that were subsequently incubated in dispase for 40 min at 37°C. Epidermal sheets were separated from the dermis and fixed in Antigen Fix (Microm Microtech) for 20 min, washed in phosphate buffer, and stained for Langerin expression. Immunofluorescence confocal microscopy was performed with a LSM 780 confocal microscope (Carl Zeiss). Separate images were collected for each fluorochrome and overlaid to obtain a multicolor image. Final image processing was performed with Imaris software (Bitplane) and Photoshop (Adobe).

**Flow cytometry.** Epidermal sheets were prepared according to the previous section and incubated in collagenase I (Life Technologies) for 30 min at 37°C. Cells were blocked with 2-4G2 for 15 min at 4°C and stained with the indicated antibodies in PBS 1% FCS 2 mM EDTA for 45 min at 4°C. Data were acquired on FACS-LSRII UV (BD) and were analyzed on DIVA software (BD). For EDU experiments, mice were injected i.p. with 1 mg of EDU and killed 14 h later. Epidermal LCs were enriched using CD45$^+$ microbeads (Miltenyi Biotec), and EDU was detected using Click-iT EDU flow cytometry assay kit (Life Technologies).

**Online supplemental material.** Fig. S1 shows quantification of the clustering index and significance evaluation. Online supplemental material is available at http://www.jem.org/cgi/content/full/jem.20130403/DC1.

We thank Jean Livet for providing the Brainbow 1.0L construct and the ImagImm photonic microscopy facility of the CIML.

This work was supported by grants from the Agence Nationale de la Recherche (ANR) ANR-08-JCJC-0134 and ANR-10-INBS-04-01 France Bio Imaging and the Human Frontier Science Program (Young Investigator Grant RGY0077/2011). The generation of Langerin-Cre mice was supported by a grant from the Netherlands Organization for Scientific Research (NWO, VIDI 917-76-365).

The authors have no conflicting financial interests.

Author contributions: C. Ghigo, I. Mondor, A. Jorquera, S. Wienert, and J. Nowak performed the experiments. S.P. Zahner and B.E. Clausen developed and provided Langerin-Cre mice. H. Luche and B. Malissen provided technical help for the design of the Ubow construct. F. Klauschen and M. Bajénoff designed the experiments and wrote the manuscript.

**Submitted: 22 February 2013**
**Accepted: 23 July 2013**

## REFERENCES

Borkowski, T.A., J.J. Letterio, A.G. Farr, and M.C. Udey. 1996. A role for endogenous transforming growth factor β1 in Langerhans cell biology: the skin of transforming growth factor β1–null mice is devoid of epidermal Langerhans cells. *J. Exp. Med.* 184:2417–2422. http://dx.doi.org/10.1084/jem.184.6.2417

Borkowski, T.A., J.J. Letterio, C.L. Mackall, A. Saitoh, A.G. Farr, X.J. Wang, D.R. Roop, R.E. Gress, and M.C. Udey. 1997. Langerhans cells in the TGF beta 1 null mouse. *Adv. Exp. Med. Biol.* 417:307–310.

Carreno, B.M., and M. Collins. 2002. The B7 family of ligands and its receptors: new pathways for costimulation and inhibition of immune responses. *Annu. Rev. Immunol.* 20:29–53. http://dx.doi.org/10.1146/annurev.immunol.20.091101.091806

Chorro, L., A. Sarde, M. Li, K.J. Woollard, P. Chambon, B. Malissen, A. Kissenpfennig, J.B. Barbaroux, R. Groves, and F. Geissmann. 2009. Langerhans cell (LC) proliferation mediates neonatal development, homeostasis, and inflammation-associated expansion of the epidermal LC network. *J. Exp. Med.* 206:3089–3100. http://dx.doi.org/10.1084/jem.20091586

Ginhoux, F., F. Tacke, V. Angeli, M. Bogunovic, M. Loubeau, X.M. Dai, E.R. Stanley, G.J. Randolph, and M. Merad. 2006. Langerhans cells arise from monocytes in vivo. *Nat. Immunol.* 7:265–273. http://dx.doi.org/10.1038/ni1307

Girolomoni, G., J.C. Simon, P.R. Bergstresser, and P.D. Cruz Jr. 1990. Freshly isolated spleen dendritic cells and epidermal Langerhans cells undergo similar phenotypic and functional changes during short-term culture. *J. Immunol.* 145:2820–2826.

Greter, M., I. Lelios, P. Pelczar, G. Hoeffel, J. Price, M. Leboeuf, T.M. Kündig, K. Frei, F. Ginhoux, M. Merad, and B. Becher. 2012. Stroma-derived interleukin-34 controls the development and maintenance of langerhans cells and the maintenance of microglia. *Immunity*. 37:1050–1060. http://dx.doi.org/10.1016/j.immuni.2012.11.001

Holzmann, S., C.H. Tripp, M. Schmuth, K. Janke, F. Koch, S. Saeland, P. Stoitzner, and N. Romani. 2004. A model system using tape stripping for characterization of Langerhans cell-precursors in vivo. *J. Invest. Dermatol.* 122:1165–1174. http://dx.doi.org/10.1111/j.0022-202X.2004.22520.x

Irion, S., H. Luche, P. Gadue, H.J. Fehling, M. Kennedy, and G. Keller. 2007. Identification and targeting of the ROSA26 locus in human embryonic stem cells. *Nat. Biotechnol.* 25:1477–1482. http://dx.doi.org/10.1038/nbt1362

Kel, J.M., M.J. Girard-Madoux, B. Reizis, and B.E. Clausen. 2010. TGF-beta is required to maintain the pool of immature Langerhans cells in

the epidermis. *J. Immunol.* 185:3248–3255. http://dx.doi.org/10.4049/jimmunol.1000981

Kouskoff, V., H.J. Fehling, M. Lemeur, C. Benoist, and D. Mathis. 1993. A vector driving the expression of foreign cDNAs in the MHC class II-positive cells of transgenic mice. *J. Immunol. Methods*. 166:287–291. http://dx.doi.org/10.1016/0022-1759(93)90370-M

Liu, K., C. Waskow, X. Liu, K. Yao, J. Hoh, and M. Nussenzweig. 2007. Origin of dendritic cells in peripheral lymphoid organs of mice. *Nat. Immunol.* 8:578–583. http://dx.doi.org/10.1038/ni1462

Livet, J., T.A. Weissman, H. Kang, R.W. Draft, J. Lu, R.A. Bennis, J.R. Sanes, and J.W. Lichtman. 2007. Transgenic strategies for combinatorial expression of fluorescent proteins in the nervous system. *Nature*. 450:56–62. http://dx.doi.org/10.1038/nature06293

McKenna, H.J., K.L. Stocking, R.E. Miller, K. Brasel, T. De Smedt, E. Maraskovsky, C.R. Maliszewski, D.H. Lynch, J. Smith, B. Pulendran, et al. 2000. Mice lacking flt3 ligand have deficient hematopoiesis affecting hematopoietic progenitor cells, dendritic cells, and natural killer cells. *Blood*. 95:3489–3497.

Merad, M., M.G. Manz, H. Karsunky, A. Wagers, W. Peters, I. Charo, I.L. Weissman, J.G. Cyster, and E.G. Engleman. 2002. Langerhans cells renew in the skin throughout life under steady-state conditions. *Nat. Immunol.* 3:1135–1141. http://dx.doi.org/10.1038/ni852

Merad, M., F. Ginhoux, and M. Collin. 2008. Origin, homeostasis and function of Langerhans cells and other langerin-expressing dendritic cells. *Nat. Rev. Immunol.* 8:935–947. http://dx.doi.org/10.1038/nri2455

Nagao, K., T. Kobayashi, K. Moro, M. Ohyama, T. Adachi, D.Y. Kitashima, S. Ueha, K. Horiuchi, H. Tanizaki, K. Kabashima, et al. 2012. Stress-induced production of chemokines by hair follicles regulates the trafficking of dendritic cells in skin. *Nat. Immunol.* 13:744–752. http://dx.doi.org/10.1038/ni.2353

Poulin, L.F., S. Henri, B. de Bovis, E. Devilard, A. Kissenpfennig, and B. Malissen. 2007. The dermis contains langerin+ dendritic cells that develop and function independently of epidermal Langerhans cells. *J. Exp. Med.* 204:3119–3131. http://dx.doi.org/10.1084/jem.20071724

Ruzankina, Y., C. Pinzon-Guzman, A. Asare, T. Ong, L. Pontano, G. Cotsarelis, V.P. Zediak, M. Velez, A. Bhandoola, and E.J. Brown. 2007. Deletion of the developmentally essential gene ATR in adult mice leads to age-related phenotypes and stem cell loss. *Cell Stem Cell*. 1:113–126. http://dx.doi.org/10.1016/j.stem.2007.03.002

Snippert, H.J., L.G. van der Flier, T. Sato, J.H. van Es, M. van den Born, C. Kroon-Veenboer, N. Barker, A.M. Klein, J. van Rheenen, B.D. Simons, and H. Clevers. 2010. Intestinal crypt homeostasis results from neutral competition between symmetrically dividing Lgr5 stem cells. *Cell*. 143:134–144. http://dx.doi.org/10.1016/j.cell.2010.09.016

Tabansky, I., A. Lenarcic, R.W. Draft, K. Loulier, D.B. Keskin, J. Rosains, J. Rivera-Feliciano, J.W. Lichtman, J. Livet, J.N. Stern, et al. 2013. Developmental bias in cleavage-stage mouse blastomeres. *Curr. Biol.* 23:21–31. http://dx.doi.org/10.1016/j.cub.2012.10.054

Vishwanath, M., A. Nishibu, S. Saeland, B.R. Ward, N. Mizumoto, H.L. Ploegh, M. Boes, and A. Takashima. 2006. Development of intravital intermittent confocal imaging system for studying Langerhans cell turnover. *J. Invest. Dermatol.* 126:2452–2457. http://dx.doi.org/10.1038/sj.jid.5700448

Wang, Y., K.J. Szretter, W. Vermi, S. Gilfillan, C. Rossini, M. Cella, A.D. Barrow, M.S. Diamond, and M. Colonna. 2012. IL-34 is a tissue-restricted ligand of CSF1R required for the development of Langerhans cells and microglia. *Nat. Immunol.* 13:753–760. http://dx.doi.org/10.1038/ni.2360

Wienert, S., D. Heim, M. Kotani, B. Lindequist, A. Stenzinger, M. Ishii, P. Hufnagl, M. Beil, M. Dietel, C. Denkert, and F. Klauschen. 2013. CognitionMaster: an object-based image analysis framework. *Diagn. Pathol.* 8:34.

Waskow, C. 2010. Generation of parabiotic mice for the study of DC and DC precursor circulation. *Methods Mol. Biol.* 595:413–428. http://dx.doi.org/10.1007/978-1-60761-421-0_27

Zahner, S.P., J.M. Kel, C.A. Martina, I. Brouwers-Haspels, M.A. van Roon, and B.E. Clausen. 2011. Conditional deletion of TGF-βR1 using Langerin-Cre mice results in Langerhans cell deficiency and reduced contact hypersensitivity. *J. Immunol.* 187:5069–5076. http://dx.doi.org/10.4049/jimmunol.1101880

Zhang, Y., J.P. Muyrers, G. Testa, and A.F. Stewart. 2000. DNA cloning by homologous recombination in Escherichia coli. *Nat. Biotechnol.* 18:1314–1317. http://dx.doi.org/10.1038/78475